Geosci. Model Dev. Discuss., 6, 791–840, 2013
www.geosci-model-dev-discuss.net/6/791/2013/
doi:10.5194/gmdd-6-791-2013

Geoscientific Model Development Discussions
Open Access

Sensitivities and uncertainties of modeled ground temperatures in mountain environments

S. Gubler, S. Endrizzi, S. Gruber, and R. S. Purves

Department of Geography, University of Zurich, Zurich, Switzerland

Received: 19 December 2012 – Accepted: 26 January 2013 – Published: 6 February 2013

Correspondence to: S. Gubler (stefanie.gubler@geo.uzh.ch)

Published by Copernicus Publications on behalf of the European Geosciences Union.

Abstract

Before operational use or for decision making, models must be validated, and the degree of trust in model outputs should be quantified. Often, model validation is performed at single locations due to the lack of spatially-distributed data. Since the analysis of parametric model uncertainties can be performed independently of observations, it is a suitable method to test the influence of environmental variability on model evaluation. In this study, the sensitivities and uncertainty of a physically-based mountain permafrost model are quantified within an artificial topography consisting of different elevations and exposures combined with six ground types characterized by their hydraulic properties. The analyses performed for all combinations of topographic factors and ground types allowed to quantify the variability of model sensitivity and uncertainty within mountain regions.

We found that modeled snow duration considerably influences the mean annual ground temperature (MAGT). The melt-out day of snow (MD) is determined by processes determining snow accumulation and melting. Parameters such as the temperature and precipitation lapse rate and the snow correction factor have therefore a great impact on modeled MAGT. Ground albedo changes MAGT from 0.5 to 4 °C in dependence of the elevation, the aspect and the ground type. South-exposed inclined locations are more sensitive to changes in ground albedo than north-exposed slopes since they receive more solar radiation. The sensitivity to ground albedo increases with decreasing elevation due to shorter snow cover. Snow albedo and other parameters determining the amount of reflected solar radiation are important, changing MAGT at different depths by more than 1 °C. Parameters influencing the turbulent fluxes as the roughness length or the dew temperature are more sensitive at low elevation sites due to higher air temperatures and decreased solar radiation. Modeling the individual terms of the energy balance correctly is hence crucial in any physically-based permafrost model, and a separate evaluation of the energy fluxes could substantially improve the results of permafrost models. The sensitivity in the hydraulic properties change

GMDD
6, 791–840, 2013

considerably for different ground types: rock or clay for instance are not sensitive while gravel or peat, accurate measurements of the hydraulic properties could significantly improve modeled ground temperatures. Further, the discretization of ground, snow and time have an impact on modeled MAGT that cannot be neglected (more than 1 °C for several discretization parameters). We show that the temporal resolution should be at least one hour to ensure errors less than 0.2 °C in modeled MAGT, and the uppermost ground layer should at most be 20 mm thick.

Within the topographic setting, the total parametric output uncertainties expressed as the standard deviation of the Monte Carlo model simulations range from 0.1 to 0.5 °C for clay, silt and rock, and from 0.1 to 0.8 °C for peat, sand and gravel. These uncertainties are comparable to the variability of ground surface temperatures measured within 10 m × 10 m grids in Switzerland. The increased uncertainties for sand, peat and gravel is largely due to the high hydraulic conductivity.

1 Introduction

Models are important tools for investigating natural processes and providing scenarios relating to future environments. Physically-based or empirical models can predict spatial or temporal variation of measured attributes and related phenomena of interest, and derived products may serve as a basis for political or economical decisions. To enhance trust in conclusions based on simulations and in data products based on predictions, a model's fit for the intended purpose must be evaluated (Rykiel, 1996). Model evaluation forms an important part of the development process (e.g. Beven, 1993; Gupta et al., 2005).

It aims at:

1. Determining the degree of accordance of a model output with the respective measured quantity (e.g. Rykiel, 1996; Beck et al., 1997; Anderson and Bates, 2001; Stow et al., 2009),

GMDD
6, 791–840, 2013

2. Quantifying the related model uncertainty (e.g. Beck, 1987; Beven and Binley, 1992; Beven, 1993; Davis and Keller, 1997; Crosetto and Tarantola, 2001),

3. Identifying parameters and input variables that account for the largest parts of this uncertainty (e.g. Cukier et al., 1977; Sobol, 1993; Saltelli et al., 2004, 2008) and

4. Eventually calibrating the model to local conditions (e.g. Beven and Binley, 1992; Chen et al., 2000; Gupta et al., 2005).

Uncertainties and errors come from processes that are not represented in the model, unknown physical properties, errors in input data, numerical errors, the modelers perception when selecting the processes to be represented, among others (Gupta et al., 2005). Uncertainty can be defined as limits in modeling due to lack of knowledge (e.g. unknown physical properties), while errors are due from numerical approximations, for example (AIAA, 1998).

Models are often applied to make predictions for large spatial areas. However, model evaluation is typically restricted to only one or, in the best case, a few evaluation points due to lack of observed data for validation. In turn, this implicitly assumes that validation at a single point suffices to inform decisions about model performance in different environmental conditions because the model is physically-based (and thus representativity at one point implies representativity over a domain). However, the implications of this assumption when modeling phenomena in highly variable terrain or over long distances has been the subject of limited research. This paper is focused on a sensitivity and uncertainty analysis of a physically-based mountain permafrost model to serve as a case study for examining the role of environmental variability in model evaluation.

The validity of a model cannot be determined based only on sensitivity and uncertainty analyses since the model outputs are not compared to measured values. However, model sensitivities and uncertainties can be analyzed independently of such ground truth measurements. Sensitivity and uncertainty analyses are one valuable way of exploring the potential influence of different environmental settings on model evaluation, without requiring spatially-distributed measurements. Since the processes

GMDD
6, 791–840, 2013

determining the occurrence and characteristics of mountain permafrost are highly complex and non-linear, a mountain permafrost model is a suitable tool to investigate the variability of model sensitivities and uncertainties in a highly variable environment.

The focus of this study lies on the variability of sensitivities and uncertainties for different topographic and other environmental conditions (Table 1). Here, sensitivity analysis quantifies the variation of the modeled output due to variation in single model parameters, while an uncertainty analysis quantifies the total parametric model output uncertainty due to errors or uncertainties in model parameters. A preliminary parameter calibration, i.e. an adjustment of the parameter's influence using given values for an output, is performed on selected parameters that influence snow duration most strongly. The object of investigation in this study is an energy- and mass-balance model with a primary focus on exploring variables and processes relating to permafrost, i.e. those influencing ground temperatures (GTs). GTs are interesting because they are influenced by highly non-linear environmental processes such as the energy balance at the Earth's surface, snow cover distribution and snow melting, as well as heat conduction on the ground, which is determined by the thermal properties of the ground constituents and its water content and phase state (e.g. Williams and Smith, 1989). In mountain regions, GTs are strongly coupled to air temperature in summer, and are influenced by solar radiation, snow cover in winter and the ground material (e.g. Haeberli, 1973; Hoelzle, 1996; Keller and Gubler, 1993; Luetschg et al., 2008; Gruber and Hoelzle, 2008). Within a mountainous environment, these variables and processes vary within short distances (e.g. Hoelzle et al., 2003; Gubler et al., 2011), which makes interpolation of model outputs difficult. Similarly, results obtained from model evaluation cannot simply be transferred to other locations. To summarize, the main goals of this study are:

- to examine the influence of environmental variability on model sensitivity and uncertainty, and discuss the importance of representative model evaluation,

GMDD
6, 791–840, 2013

– to quantify the sensitivity of mean annual ground temperature (MAGT) due to errors in discretization, numerical and model specific parameters and uncertainties in physical parameters, and

– to discuss the influence of environmental variability on a physically-based energy- and mass-balance model.

2 Model and data description

2.1 The energy- and mass-balance model GEOtop

GEOtop is a physically-based model originally developed for hydrological research. It couples the ground heat and water budgets, represents the energy exchange with the atmosphere, has a multilayer snow pack and represents the water and energy budget of the snow cover (Bertoldi et al., 2006; Rigon et al., 2006; Endrizzi, 2007; Dall'Amico, 2010). GEOtop simulates the temporal evolution of the snow depth and its effect on ground temperature. It solves the heat conduction equation in one dimension and the Richard's equation for water transport in one or three dimensions describing water infiltration in the ground as well as freezing and thawing processes. GEOtop is therefore a suitable tool to model permafrost relevant variables such as snow and ground temperatures (Fig. 2). It can be applied in high mountain regions and allows accounting for topographic and other environmental variability. This study is performed using the GEOtop version number 1.225-9.

2.2 Input and validation measurements

Input data consist of measured air temperature, wind velocity and direction, relative humidity, global shortwave radiation and precipitation recorded by the MeteoSwiss meteorological stations. The experiment is run at Corvatsch, Upper Engadine, Switzerland, where a meteorological station of MeteoSwiss is located at 3315 m a.s.l. A preliminary

GMDD
6, 791–840, 2013

model analysis is performed at the 40 locations of ground surface temperature measurements around Corvatsch (Gubler et al., 2011). The two main target variables are the mean annual ground surface temperature (MAGST) and the melt out date of the snow (MD) (Schmid et al., 2012). The study was performed for two years of data, i.e. from summer 2009 to summer 2011.

2.3 Model parameters

2.3.1 Numerical parameters

In GEOtop, ground discretization is given as the thickness dz of each ground layer. Close to the surface, the ground is resolved in finer detail due to the greater temperature gradients. To reduce the number of degrees of freedom, the thickness of the ground layers is parameterized as an exponential function, describing the ground layer i as:

$$dz_i = dz_{\min} \cdot (1 + b)^{i-1}, \tag{1}$$

where $dz_{\min}$ is the thickness of the first layer, b is the growth rate and i is the layer index, being one at the ground surface and increasing downwards. In addition, the maximal depth $z_{\max}$ of the modeled ground must be set as a parameter.

Snow resolution is higher close to the snow surface (snow-atmosphere interface) and to the ground (snow-ground interface). A snow portion at the top (referred to as top region) and at the bottom (bottom region) are defined that are discretized with snow layers that never exceed a specified snow water equivalent (swe_m). The top and bottom regions are defined by their maximum snow water equivalent content, respectively given by $n_t \cdot \mathrm{swe}_m$ and $n_b \cdot \mathrm{swe}_m$, where n_t and n_b are integers. On the other hand, the portion of the snow pack not included in the top and bottom regions constitutes the middle region, which is discretized with a maximum number n_m of layers with minimum snow water equivalent content equal to swe_m and no maximum. The layering algorithm

GMDD
6, 791–840, 2013

prevents the formation of significant snow water equivalent differences across the layers when the value swe_m is exceeded.

The heat and Richards' equations are solved with the Newton Raphson method (Kelley, 2003). Significant numerical parameters are the time step dt of numerical integration of the equations and the residual tolerance at which the iterations are terminated. The sensitivity of the GEOtop model to both these parameters are also quantified in this study. The time step has been made to vary in the range from 7.5 min to 4 h. The higher the time step and residual tolerance are, the longer the computing time is. The optimal parameters for the simulation are the highest time step and residual tolerance for which a decrement of their value does not result in a significant numerical solution difference.

2.3.2 Model specific parameters

An initial condition of the state variables, namely temperature and total (= ice + liquid water) soil moisture initial profiles, must be assigned to run the model. Since there is always a certain degree of arbitrariness in that, the simulations are then run for a long time so that they lose memory of the initial values and will assume values in equilibrium with the meteorological forcings and the ground properties. However, different responses may take place if the initial condition is given by unfrozen and frozen ground. Therefore, both the initial conditions of initial ground temperatures at 1 °C and −1 °C are considered. The initial total soil moisture profile is obtained from the retention curve after assigning an hydrostatic water pressure profile, and then the total soil moisture in ice and liquid water are split according to ground temperature and the freezing soil characteristic curve (e.g. Dall'Amico, 2010).

Although this study deals with one-dimensional simulations, it is possible to represent lateral water drainage between the surface and a depth referred to as z_f, while below this depth the ground can be filled with water until it is saturated. In dependence of the modelers interest, the *water balance* can be turned off if no information on the ground

GMDD
6, 791–840, 2013

hydraulic properties are available, to save computation time or to study the influence of water balance on model outputs.

The *longwave downward radiation* (LDR) parameterizations implemented in GEOtop are based on the Stefan Boltzmann law:

$$\mathrm{LWR_{in}} = \epsilon_{\mathrm{atm}} \cdot \sigma_{\mathrm{SB}} \cdot T_{\mathrm{atm}}^4, \tag{2}$$

where $\sigma_{\mathrm{SB}} = 5.67 \cdot 10^{-8}\,\mathrm{W\,m^{-2}\,K^{-4}}$ denotes the Stefan-Boltzmann constant, ϵ_{atm} the bulk emissivity and T_{atm} the effective temperature of the overlying atmosphere. In practice, T_{atm} is replaced by the temperature at screen-level height temperature T, and the atmospheric emissivity is parameterized as a function of air temperature and/or vapor pressure. Diverse LDR parameterizations can be found in the literature (Brutsaert, 1975; Idso, 1981; Konzelmann et al., 1994; Prata, 1996, among others). GEOtop includes a switch to select one out of nine parameterizations. Gubler et al. (2012) calibrated these parameterizations to measured longwave radiation in Switzerland. The sensitivity on the different LDR parameterizations, as well as on the calibrated Konzelmann et al. (1994) parameterization is tested.

The turbulent fluxes of sensible and latent heat are calculated using the *Monin-Obukhov similarity theory* (Obukhov, 1946; Monin and Obukhov, 1954), which represents the effect of buoyancy with corrections to the logarithm profile of wind speed, valid only in a neutral atmosphere. However, the theory only determines the functional dependence of the corrections. Their mathematical formulation has to be found empirically. For this reason, in the present study the possibility to represent the turbulent fluxes assuming a neutral atmosphere is also considered. This becomes very important when the atmosphere is stable, because in this case the Monin-Obukhov corrections may improperly suppress turbulence and, as a result, the surface may be de-coupled from the atmosphere, originating significant errors. If the wind speed is very small, such de-coupling may also occur. Therefore, a minimum wind speed (V_{min}) has been added as a parameter. A minimum relative humidity ($\mathrm{RH_{min}}$) has also been added to prevent unrealistic turbulent fluxes. The *temperature threshold for rain* $T_{r,\,0}$ (respectively *snow*

GMDD
6, 791–840, 2013

$T_{s,0}$) determines the temperature above (below) which all precipitation is rain (snow). Between the two thresholds, the amount of precipitation being rain or snow is interpolated linearly. They are set from 0 to 4 °C for rain, and −3 to 0 °C for snow.

2.3.3 Physical parameters

The parameters considered for ground are its aerodynamical roughness, ground albedo and emissivity, as well as its hydraulic properties presented in Sect. 2.4.2. The ground roughness influences the turbulent fluxes, and ranges from few millimeters up to half a meter or more in dependence of terrain obstacles (Wieringa, 1993). The albedo of a dry ground surface $\alpha_{\mathrm{g,\,dry}}$ is assumed to range from 0.1 to 0.4, values that are typically found in the literature (e.g. Ångström, 1925; Tetzlaff, 1983; Ineichen et al., 1990; Scharmer and Greif, 2000; Markvart and Castañer, 2003; Polo et al., 2012), with an average of 0.2. The reflection of wet ground $\alpha_{\mathrm{g,\,wet}}$ is smaller than the one for dry ground (Ångström, 1925), modeled as:

$$\alpha_{\mathrm{g,\,wet}} = \frac{\alpha_{\mathrm{g,\,dry}}}{f_{\alpha_{\mathrm{g,\,wet}}}}, \tag{3}$$

where $0.4 \leq f_{\alpha_{\mathrm{g,\,wet}}} \leq 1$ is the divisor used to model wet ground albedo. Emissivity of the different ground types is assumed between 0.8 and 0.99 with an average of 0.96 (e.g. Sutherland, 1986; Ogawa and Schmugge, 2004; Jin and Shunlin, 2006). The heat flux at the bottom of the ground profile determines the lower boundary condition of the heat conduction. The deep ground heat flux is 0.07 $\mathrm{W\,m^{-2}}$ (Medici and Rybach, 1995). Due to geometrical effects in high mountain regions the density of the ground heat flux in complex topographies varies (Kohl, 1999; Nötzli et al., 2007), and is hence assumed to have an average value of 0.05.

Diverse parameters concerning snow such as the snow reflectance, its emissivity, roughness, viscosity and the snow compaction rate can be set in GEOtop, determining the outgoing longwave radiation, the turbulent fluxes and the snow densification,

GMDD
6, 791–840, 2013

They influence snow melt and the duration of the snow cover in spring. For shallow snow-packs, snow albedo decreases since a significant portion of incoming shortwave radiation is actually absorbed by the ground surface (Tarboton and Luce, 1996). In GEOtop, this is represented by the *albedo extinction parameter* c_α. If the snow height z is smaller than c_α, ground and snow albedo are linearly interpolated. Snow emissivity ranges from 0.94 to 0.99 with an baseline value of 0.98 (e.g. Dozier and Warren, 1982; Zhang, 2005; Hori et al., 2006). The albedo of fresh snow for visible light is between 0.8 and 0.96 (e.g. Markvart and Castañer, 2003). The uncertainties in the atmospheric parameters that determine the attenuation of solar radiation are according to Gubler et al. (2012).

2.3.4 Input measurements and extrapolation

Air temperature is extrapolated at different elevations using a lapse rate. Analogous to air temperature, dew temperature and precipitation are also distributed at different elevations using an elevation-related lapse rate. Precipitation measurements can have a negative bias due to wetting loss or wind-induced under-catch (Legates and DeLiberty, 1993; Goodison et al., 1998), for example. To deal with this systematic measurement error which has great effects on snow accumulation and soil moisture, GEOtop considers a *precipitation correction factor* multiplying the precipitation measurement.

The *height of the sensor* at which a temperature or wind speed are measured influences the calculation of the turbulent fluxes. While the exact height of the meteorological station can be measured precisely, the topography of the station in mountain regions may influence the height equivalent considering an infinite planar surface (Fig. 3). In this study, the height varies between 0.5 and 16 m to model both valley and top of mountain situations.

GMDD
6, 791–840, 2013

2.4 Experimental setting

The sensitivity study is performed for six different ground types (Sect. 2.4.2), that are varied within a topographical setting typical for mountain areas (Table 3). GEOtop is run for all combinations of ground types and topographical attributes that are assumed important when modeling mountain permafrost. The influence of environmental variability on model sensitivities and uncertainties is quantified.

2.4.1 Topography

The modeling study is performed within an artificial set of topographic attributes to evaluate the sensitivities of GEOtop for diverse topographical situations (Table 3). We model elevations in steps of 500 m from 500 to 4000 m a.s.l. Slope varies from zero degrees to thirty degrees in steps of ten degrees, and aspect is varied in steps of 45 degrees, thereby covering the most important exposure to the sun. In total, this topography sampling results in 200 simulation points, respectively 328 for rock, resulting in a total of 1328 simulation points. All locations where snow did not melt in summer were excluded from the analysis.

2.4.2 Ground types

Different ground types and ground surface covers influence the ground thermal regime substantially. Liquid water influences the thermal conductivity of the ground as well as the latent heat transfer during freezing and thawing of a specific ground layer (Williams and Smith, 1989). The study was performed for six different ground types: clay, sand, silt, peat, gravel and rock. For each of these ground types, typical values for the residual water content θ_r, the saturated water content θ_s, the parameters n_{vG} and α_{vG} determining the shape of the water retention curve parameterized according to van Genuchten (1980) and the saturated hydraulic conductivity K_h are determined (Table 4). The lateral hydraulic conductivity is assumed to be the same as the normal hydraulic conductivity.

GMDD
6, 791–840, 2013

The thermal conductivity K_T is set to $2.5\,\mathrm{W\,m^{-1}\,K^{-1}}$ and the thermal capacity C of the mineral particles to $2.25 \times 10^6\,\mathrm{J\,m^{-3}\,K^{-1}}$ for the mineral particles (e.g. Cermák and Rybach, 1982; Wegmann et al., 1998; Šafanda, 1999). Ground is defined here as the volume below the Earth's surface for which temperature is studied.

The parameter values for silt, sand and clay are taken from Twarakavi et al. (2010, Table 2). For peat, the parameter values come from Carey et al. (2007); Quinton et al. (2008, Table 2). Residual and saturated water content for gravel is assumed to be similar to sand. The van Genuchten parameters and the hydraulic conductivity for gravel are approximated from Maier et al. (2009). For rock, they are assumed to be the same as for clay, and the hydraulic conductivity, and θ_r and θ_s are assumed to be very small. Measurements of the van Genuchten parameters for rock were not found in the literature.

2.5 Target variable

Ground temperatures are linearly interpolated between the simulation nodes that represent layers in the numerical scheme. Thereby, the modeled MAGT are compared at the same depths. The annual mean, minimum and maximum values at 10 cm, 1 m, 5 m and 10 m depth are estimated.

3 Experiments

This sensitivity and uncertainty study was performed based on the energy- and mass-balance model GEOtop (Rigon et al., 2006) (Sect. 2.1). A local sensitivity analysis (Sect. 4.2) on individual parameters was performed with a special focus on variations within topographically variable terrain (Sect. 2.4.1). Then, a subset of sensitive physical parameters was selected to quantify the total parametric output uncertainty of GEOtop (Sect. 3.3).

GMDD
6, 791–840, 2013

3.1 Preliminary analysis

The parameters that predominantly influence the duration of snow cover were calibrated in a preliminary analysis, since snow exerts great influence on ground temperatures through insulation (Zhang, 2005; Goodrich, 1982). The error of simulated melt-out day (MD) is compared to MD observed at 39 locations around the Corvatsch mountain (Gubler et al., 2011; Schmid et al., 2012). MD is simulated for diverse parameter sets obtained by globally varying the most important parameters which are influencing MD. The simulations are calibrated to determine the most plausible parameter values.

3.2 Sensitivity analysis

A model can be regarded as a black box represented by a function $f(x_1, x_2, ..., x_n) = (y_1, y_2, ..., y_m)$, where $(x_1, x_2, ..., x_n)$ are the model parameters and $(y_1, y_2, ..., y_m)$ are the model outputs. To evaluate GEOtop, a sensitivity analysis on 52 individual parameters is performed to (a) quantify the influence of each parameter on the output variables of interest, and (b) to determine the most important physical parameters for the subsequent uncertainty analysis. The sensitivity of a parameter x_j is determined by keeping all parameters $x_i, i \neq j$ fixed at their baseline value $X_{j0} = (x_{10}, x_{20}, ..., x_{(j-1)0}, x_{(j+1)0}, ..., x_{n0})$, and varying x_j within its plausible range. The ranges of the parameters are determined based on literature review and/or expert opinion. The variation of the model outputs $y_k, k = 1, ..., m$ is evaluated, and local sensitivities $s_{j,k}$ are quantified, defined here as the range of the 95 % of the simulated outputs.

The parameters are categorized into (a) very sensitive parameters, (b) sensitive parameters and (c) non-sensitive parameters. Category (a) includes all parameters that are tuned in a preliminary analysis (Sect. 3.1). The second category includes all parameters having non-negligible influence to the model outputs. All physical parameters changing MAGT by at least 0.5 °C in the sensitivity analysis are included in the uncertainty analysis.

GMDD
6, 791–840, 2013

3.3 Uncertainty analysis

A prior distribution is assigned to each of the selected physical parameters. If a parameter has only positive values, it is assumed to be log-normally distributed, otherwise it follows a normal distribution. All parameters are assumed independent. Since the study setting is synthetic, spatial autocorrelation of the parameters are not taken into account. The location parameter is the average of the parameter values determined for the local sensitivity analysis (e.g. Table 1), and the standard deviation is chosen such that the range encloses 95 % of the values for a normally distributed parameter. If a parameter is log-normally distributed (e.g. $x \sim \mathcal{L}(\mu, \sigma^2)$), the expected value $\mathrm{E}[X]$ is the baseline value , and the variance $\mathrm{Var}[X]$ is chosen appropriately representing the variability of the parameter. The statistical parameters of the log-normal distribution are:

$$\sigma = \log\left(\frac{\mathrm{Var}[X]}{\mathrm{E}[X]} + 1\right) \tag{4}$$

$$\mu = \log(\mathrm{E}[X]) - \frac{\sigma^2}{2}. \tag{5}$$

Each parameter is sampled according to its prior distribution, and a GEOtop simulation is performed for each parameter set. In total, 1500 model simulations are performed to ensure convergence of the output probability distribution (Fig. 10). The results are depicted as relative frequency histograms to evaluate the total model output uncertainty, and are quantified as the standard deviation of the model output distribution.

3.4 Model simulations

The sensitivity and uncertainty analyses are performed systematically for different ground types within a setting representing the topographic variability encountered in mountain regions (Sect. 2.4). In total, 1328 locations are simulated. For the sensitivity analysis, a number of 256 simulations are performed per location. The uncertainty

GMDD
6, 791–840, 2013

analysis requires 1500 simulations to reach convergence per location. In total, more than two million GEOtop simulations are performed. The simulations are visually analyzed using small-multiple plots (Tufte, 1983, 1990) (e.g. Fig. 7), and summarized in boxplots for the different locations and ground types.

4 Results

4.1 Preliminary analysis

A preliminary analysis was conducted to extract reasonable values of the parameters that most considerably influence snow duration (MD). The temperature and precipitation lapse rates and the snow correction factor were calibrated using MD observations around Corvatsch (Gubler et al., 2011; Schmid et al., 2012). Due to compensating effect, different parameter combinations lead to similar results (Fig. 4). We chose to set the temperature lapse rate to its most commonly used value $-6.5\,^{\circ}\mathrm{C\,km^{-1}}$, resulting in a optimal precipitation lapse rate of $0.2\,\mathrm{km^{-1}}$ and a snow correction factor of 2 (Fig. 4). That results in an average MD error of zero days with a mean root squared error of less than 20 days for both study years 2010/2011. Precipitation lapse rate in mountain areas are normally negative accounting for greater snow accumulation in high elevation areas (e.g. Barringer, 1989). Downward transportation of snow by avalanches or wind in the study area, which is not represented in GEOtop, may be the reason for the positive precipitation lapse rate. The sensitivity to different LDR parameterizations was reduced using the calibration performed by Gubler et al. (2012).

4.2 Summarized sensitivities

4.2.1 Topographic setting

MAGT sensitivities at different depths correlate strongly, and hence all the presented results concern MAGT modeled at 1 m depth. The sensitivities to the individual

GMDD
6, 791–840, 2013

parameters *vary strongly* for different topographic factors (Fig. 5). Differences in *the temperature lapse rate* Γ_T of 2 °C km^{-1} (5.5 to 7.5 °C km^{-1}) result in maximal ground temperature differences of up to 5 °C for a elevation distances of 1000 m between the modeled location and the meteorological station, while the minimal sensitivity to Γ_T is less than 0.2 °C at locations of similar elevation as the meteorological station. Sensitivity to temperature lapse rate increases linearly with the distance to the meteorological station.

The sensitivity to the dry ground albedo increases at south exposed slopes that receive more solar radiation than adjacent slopes exposed to the north (Fig. 7). Further, low elevation sites are more sensitive to the dry ground albedo since the snow duration is shorter. The opposite is the case for the snow albedo which has an enhanced sensitivity in high elevations. The sensitivity to ground roughness, the height at which wind velocity is measured, and the dew temperature lapse rate increase for decreasing elevations. That indicates the increased importance of the turbulent fluxes in the energy balance for locations of increasing air temperatures and decreasing solar radiation.

4.2.2 Discretization errors

The thickness of the first layer $dz_{\min}$ increases linearly with increasing $dz_{\min}$ for ground type sand, peat and gravel (Fig. 6). For clay, silt and rock, the sensitivity to $dz_{\min}$ increases for $dz_{\min} \geq 40$ mm. Below that value, the sensitivity is zero for these ground types. The sensitivity to $dz_{\min}$ is smaller for MAGST close to zero degrees, i.e. at high elevations. The highest sensitivities to $dz_{\min}$ are obtained for peat, gravel and rock (Fig. 9) resulting in changes of almost 4 °C for rock. The median sensitivity to $dz_{\min}$ is relatively small up to 20 to 40 mm (Fig. 8, bottom right figure) for all environmental conditions studied here, and increases linearly for greater values. The maximal ground thickness $z_{\max}$ is not sensitive, except for few locations for rock. The *ground exponent b* is insensitive to all ground types and topographic settings. The time step for which the numerical equations are solved results in maximal MAGT differences of 0.9 to 1.3 °C changes. The minimal sensitivity to the time step is around 0.2 °C. The sensitivity to

GMDD
6, 791–840, 2013

the time step is negligible up to 15 min time resolution, and increases linearly with increasing time discretization (Fig. 8, top left figure). If computation time is no issue, the heat conduction and the Richard's equation should be solved at maximally half an hour resolution, whereas an hourly resolution leads to average differences of around 0.2 °C. The sensitivity to dt increases linearly with increasing dt, with changes of 0.8 °C for a resolution of four hours in average. The number of top layers in the snow module should be set to at least two, and the maximal value of swe_m should not exceed 10 mm to ensure stable ground temperatures. A few individual locations react non-linearly to changes in the snow discretization parameters. We were however not able to explain the non-linear response at these individual points. All discretization parameters converge to stable solutions with average errors between 0.001 and 0.06 between the finest resolutions allowing quantification of average discretization errors (Table 5). The initial ground temperature is insensitive under all environmental conditions, indicating that the ground initialization is reliable.

4.2.3 Model specific parameters

Calibration of the *LDR parameterization* by Konzelmann et al. (1994) results in a sensitivity from 0.6 to 1.2 °C within the environmental setting with respect to the published, original value of the parameterization. In sandy ground, neglecting the water balance results in changes of 1.5 °C GST. For rock or clay, the water balance is not important, and could be neglected to save computational time. The *Richard tolerance* influencing the convergence of the Richard's equation for movement of liquid water in ground is important in gravel (more than 0.5 °C), whereas for the other ground types it is insignificant. When modeling ground with great hydraulic conductivity, the tolerance of the Richard's equation should be set sufficiently small.

GMDD
6, 791–840, 2013

4.2.4 Physical parameters influencing the energy balance

The most sensitive physical parameter is the dry ground albedo. Depending on the location, the sensitivity to the dry ground albedo (0.1 to 0.4) varies from around 0.5 to more than 2.5 °C for clay, for example. It is greatest at south exposed slopes, and decreases by around 1.3 °C at north exposed slopes. A slight decrease of the sensitivity is observed for 30 degrees steep slopes facing north, while 30 degrees south facing slopes are more sensitive than flat slopes. The increased sensitivity is in direct relation to the amount of solar radiation received at a locations. The sensitivity to the dry ground albedo increases strongly with decreasing elevation for all ground types because the snow duration is shorter. The minimal MAGT change is 0.5 °C at high elevation, inclined north exposed slopes, while the maximal sensitivity to the dry ground albedo varies from 2.5 (clay, silt) to almost 4 °C (rock and gravel) (Table 9). *The wet ground albedo* is less sensitive than the dry ground albedo for all ground types. It ranges from 0.2 (gravel, sand, peat) to 1.3 °C (rock). The latter is the case since in GEOtop, wet ground albedo is taken when the water content equals θ_{sat}, and since θ_{sat} is very small in rock, that happens more quickly than for other ground types. That simplification leads to the greater sensitivity of rock to the wet ground albedo, which in reality is likely not the case. The *snow height for which the snow-ground albedo is interpolated* has a maximal sensitivity of more than 1 °C, very similar to the *fresh snow albedo*. In summary, the surface albedo determined either by snow, ground or a composition of both has the greatest influence on MAGT. That supports the importance of the solar radiation in the energy balance determining snow melt and the available energy warming the ground in this environment.

Ground roughness maximally changes MAGT at 1 m depth by around 1.2 to 2 °C (rock). The *height of the wind velocity meteorological station*, the *Monin Obhukov parameterization* and the *dew temperature lapse rate* result in differences of around 1 °C in MAGT. Turbulent fluxes as well as longwave radiation have an increased importance at night when no radiation from the sun reaches the earth. *Snow roughness* is less

GMDD
6, 791–840, 2013

important (0.5 °C) than ground roughness since the snow surface is more homogeneous. Other parameters such as *temperature threshold for snow*, the *thermal conductivity*, the *Ångström parameter* β and *snow viscosity* change MAGT by around 0.5 °C. The remaining less important parameters have a maximal sensitivity of less than 0.5 °C for all studied locations and ground types were excluded from the subsequent comprehensive uncertainty analysis to reduce the parameter space.

4.2.5 Hydraulic properties of different ground types

The sensitivity of parameters influencing the water content in the ground such as the hydraulic conductivity K_h, the surface above which all water drains z_f, the saturated water content and the van Genuchten parameter n vary strongly for the different ground types (Fig. 9). The sensitivities range from 0.2 (rock) to 2 °C (sand and peat) differences at 1 m depth for z_f, from 0.3 (rock) to 0.5 (clay, sand, gravel) to 1.2 °C (peat) for θ_{sat}, and from 0.2 (rock) to 1.2 °C (peat) for n_{vG}.

4.3 Uncertainties in modeled MAGT

Two arguments support the parameter selection for the uncertainty analysis: (a) we exclude all numerical, discretization and model specific parameters since these parameters add to model error and not to model uncertainty and (b) include only parameters that influence ground temperature for more than 0.5 °C and at least one ground type (Fig. 9). All other parameters are fixed at their baseline value. The remaining parameters are sampled randomly according to their prior distribution (Table 1). In total, 1500 simulations were run, however 750 would suffice to ensure convergence (Fig. 10).

Parametric model output uncertainty is expressed as the standard deviation of the model simulations. The frequency histograms of modeled MAGT at one location are depicted in Fig. 11. It can be assumed to be normally distributed, and hence the standard deviation is a suitable measure to quantify the uncertainty of modeled MAGT. The parametric uncertainty varies from 0.1 to 0.5 °C for MAGT modeled in clay, silt and rock,

GMDD
6, 791–840, 2013

and increases for sand, peat and gravel (Fig. 12). This underlines the increased sensitivity of these ground types to the hydraulic properties of the ground. The parametric output uncertainty decreases for increasing elevation for all ground types, which can be attributed to the increased sensitivity to parameters influencing the energy balance at low elevation sites, i.e. the sensitivity to ground albedo or roughness (Sect. 4.2). The environmental variability of the model uncertainties is not as pronounced as in the sensitivities, but is still considerable.

Model uncertainty at the surface is comparable with variability of ground surface temperatures measured within 10 m × 10 m cells, ranging from approximately 0.25 at homogeneous grass sites to 2.5 °C in block fields, expressed as the total range (Gubler et al., 2011). If expressed as a standard deviation, we see that the fine scale environmental variability is similar to the parametric uncertainty found for modeled MAGT at 10 cm depth.

Ground temperatures at greater depths integrate over larger surface areas (Gold and Lachenbruch, 1973), and are hence expected to be less variable than at the surface. Integration over large areas is not represented by GEOtop since the heat conduction is solved in one dimension.

5 Discussion

5.1 The relevance of representative model evaluation

The synthetic environment allowed us to quantify model sensitivity and uncertainty under differing environmental conditions. The selected setting allowed quantification of the influence of individual parameters for different environmental conditions, as well as identification of locations where model sensitivities and uncertainties are largest. These findings can in turn inform future measurement campaigns by quantifying the benefit of an individual measurement. For example, spatially-distributed ground albedo measurements would, especially at low elevation and south exposed sites, strongly decrease

GMDD
6, 791–840, 2013

the uncertainty of mountain permafrost models, and result in more accurate model outputs. Other parameters are sensitive only under specific conditions, such as for example the hydraulic properties of the ground. A study on rock faces alone results in an insignificant influence of the hydraulic properties on modeled ground temperatures. Applied to other ground types such as sand, peat or gravel, this conclusion that the hydraulic properties are insignificant is wrong. Hence, evaluation of spatially-distributed models should cover the main environmental properties of the modeling domain, since otherwise, important model features could be missed. A recent study obtained similar results concerning the variability of model sensitivities and uncertainties due to differing topographic and climatic conditions for a snow model (He et al., 2011).

Thus, the presented environmental setting allowed us to draw representative conclusions about the sensitivity and uncertainties of modeled MAGT in mountain regions. The results could be extended to modeling lowland areas, where the environmental variability may be for example expressed as differences in vegetation, for example. The study contributes to the request by Gupta et al. (2008) for more representative model evaluation.

5.2 Sensitivities and uncertainties of the physically-based model GEOtop

Snow is important in determining the thermal state of the ground (Goodrich, 1982; Keller and Gubler, 1993; Ishikawa, 2003; Luetschg et al., 2008). Parameters such as the temperature lapse rate or the correction factor for the precipitation measurement strongly influence snow duration, but have opposite effects. A higher lapse rate, for example, leads to warmer air temperature at low elevation site (if the meteorological station is located above the simulated locations), and results hence in faster melt-out. This is compensated by enhanced snow accumulation due to a greater precipitation lapse rate or higher precipitation correction factor. This compensating effect between different parameters is widely known as equifinality Beven and Freer (e.g. 2000). A similar result was obtained by Essery and Etchevers (2004) for the influence of the radiative and turbulent fluxes on snow melt, for which different parameter combinations provided

GMDD
6, 791–840, 2013

equally well behaving model outputs. Combination of different measured quantities could reduce the problem and lead to arguments for model improvement if conflicting results are obtained (Essery and Etchevers, 2004). GEOtop, and probably any physically-based permafrost model, would benefit from validation with distributed time series of snow height (or SWE) to distinguish between snow accumulation and melting processes. Similarly, mountain permafrost models could benefit from individual calibration of parameters influencing the energy balance such as the roughness length (e.g. Andreadis et al., 2009) or ground albedo (e.g. Hoelzle, 1996; Gruber, 2005).

The ground albedo, which determines the net shortwave radiation at the Earth's surface in summer, was the most important parameter when modeling MAGT. The importance of ground albedo in permafrost models was already investigated by Hoelzle (1996); Ling and Zhang (2004); Gruber (2005). Similarly, snow albedo is important since it strongly influences snow melting (Etchevers et al., 2004). Here, changes in the snow albedo changed MAGT by around 1 °C. The parameters influencing the turbulent fluxes determine snow melt (e.g. Etchevers et al., 2004) and change MAGT by around 0.5 to 1.5 °C. Calibration of the Konzelmann et al. (1994) LDR parameterization (e.g. Gubler et al., 2012) changes MAGT also by around 1 °C. This supports the relevance of calibrating physically-based models (e.g. Beven and Binley, 1992; Gupta et al., 1998), and underlines the importance of evaluating individual processes separately if used in impact models.

Some of the discretization parameters such as the time step at which equations are solved, as well as the thickness of the ground and snow-pack layers change MAGT by more than 1 °C. The temporal resolution should optimally be half an hour to ensure an error of less than 0.1 °C. Thickness of the uppermost ground layer of 20 mm results in 0.1 °C difference from the smallest discretization chosen (e.g. 5 mm). The findings concerning the time step and the thickness of the uppermost soil layer are comparable to the findings by Romanovsky et al. (1997), who compared the behavior of three numerical permafrost models with analytical solutions of the heat conduction.

GMDD
6, 791–840, 2013

The sensitivity of the hydraulic parameters that determine the shape of the water retention curve varies strongly for the different ground types. For clay and rock, the sensitivity is almost negligible, while for sand or gravel, the van Genuchten parameter n, θ_{sat} and the hydraulic conductivity play a major role. Seaman et al. (2009) found that n, θ_{sat}, θ_{res} are the most important parameters to predict water retention in sand. The hydraulic conductivity K_h, θ_{sat} and θ_{res} were most important to estimate ground moisture by Mertens et al. (2005), while Jhorar et al. (2002) recommended to fit α, n and θ_{sat} when using the van Genuchten parameterization. The sensitivity of the van Genuchten parameters are hence controversial in the literature (e.g. Pollaco and Mohanty, 2012). In this study, we found that the hydraulic conductivity, the shape parameter n and the porosity most strongly influence MAGT for sand, peat and gravel. The variable sensitivity observed for the different soil types may by a reason for the controversial sensitivities found in the literature. These results underline the importance of systematic model evaluation for different environmental settings, since otherwise important model features are missed and would lead to wrong conclusions. Extrapolation of model uncertainties to locations of different environmental conditions is not feasible unless a systematic analysis spanning the environmental variability is performed.

The total parametric uncertainty, expressed as the standard deviation of the model outputs, goes from 0.1 to 0.5 °C for clay, silt and rock, and increases up to 0.7 °C for peat, sand and gravel. This underlines the importance of hydraulic properties of ground types having high hydraulic conductivity and high porosity. In general, uncertainty is greater at low elevation sites since the sensitivity to the ground albedo, as well as the turbulent fluxes increases at low elevation sites. Parametric uncertainty of MAGT at different depth is almost constant. The parametric model uncertainty is comparable to small scale environmental variability of ground surface temperatures measured in Switzerland (Gubler et al., 2011).

GMDD
6, 791–840, 2013

6 Conclusions

6.1 Environmental variability

Sensitivity and uncertainty studies are widely known to inform model use, respectively model improvement as they serve to reason whether model outputs and their uncertainties agree with our theoretical understanding of an environmental system. If a model is applied within highly variable environment, sensitivities and uncertainties can vary strongly even for locations which are spatially proximate. Considering environmental variability when analyzing model uncertainties is important to gain confidence in the conclusions made about the model and the modeled outputs. The possibility of detecting model deficiencies is higher when performing systematic and representative model evaluations. The methods we have presented in this study proved useful to study a distributed physical model used in mountain permafrost research on its uncertainties within highly variable terrain as encountered in mountain regions. The sensitivity of the model to some individual parameters proved to be highly variable. In summary, the results support the importance of systematic and representative model evaluation (e.g. Gupta et al., 2008). Further, the systematic setting allows to compare our physical understanding of the important processes to the model for a variety of test cases.

6.2 GEOtop sensitivities and uncertainties

Snow duration is strongly influenced by the processes determining snow accumulation as precipitation and redistribution by wind or avalanches, as well as melting processes determined by the available energy. Calibration and validation of modeled snow height (or SWE) at spatially-distributed locations, as well as distributed measurements of the individual components of the energy balance would provide deeper insights in the ability of GEOtop to simulate the most important processes determining the occurrence of permafrost in mountain regions. Evaluating these processes individually and independently from the heat conduction in the ground could lead to model improvement.

GMDD
6, 791–840, 2013

Measuring parameters like ground albedo would greatly improve mountain permafrost models, as it contributes most dominantly to the parametric model uncertainty. If modeling permafrost in peat or sandy ground, or in rock glaciers, precise values of the hydraulic properties of the ground could reduce model uncertainties strongly.

7 Outlook

This analyses performed in this study are of theoretical and practical relevance. The synthetic model setting allowed quantification the variability of model uncertainties within highly variable terrain as typically encountered when modeling mountain permafrost. To use GEOtop operationally, it should however be validated with spatially-distributed measurements. The diverse model parameters should be calibrated to local conditions to increase the accuracy of the model. Combination of both uncertainty and validation studies would provide additional insights on the model's ability to reproduce the processes that are relevant for mountain permafrost.

Acknowledgements. This work was supported by the AAA/SWITCH funded Swiss Multi Science Computing Grid project (www.smscg.ch) with computational infrastructure and support. Customized libraries (ggeotop and GC3Pie) and user support were kindly provided by GC3: Grid Computing Competence Center (www.gc3.uzh.ch). The authors are grateful for the support by S. Maffioletti who patiently answered to any question concerning the grid computing. This project was funded by the Swiss National Science Foundation (SNSF) via the NCCR MICS project PermaSense and via the project X-Sense (www.nano-tera.ch). All statistical analyses were performed with R (www.cran.r-project.org).

References

AIAA: Guide for the verification and validation of computational fluid dynamics simulations, American Institute of Aeronautics and Astronautics, Reston, VA, USA, 1998. 794

Anderson, M. G. and Bates, P. D. (Eds).: Model Validation: Perspectives in Hydrological Science, Wiley, New York, USA, 2001. 793

Andreadis, K. M., Storck, P., and Lettenmaier, D. P.: Modeling snow accumulation and ablation processes in forested environments, Water Resour. Res., 45, W05429, doi:10.1029/2008WR007042, 2009. 813
Ångström, A.: The albedo of various surfaces of ground, Geograf. Ann., 7, 323–342, 1925. 800
Barringer, J. R. F.: A variable lapse rate snowline model for the remarkables, Central Otago, New Zealand, J. Hydrol., 28, 32–46, 1989. 806
Beck, M. B.: Water quality modeling: a review of the analysis of uncertainty, Water Resour. Res., 23, 1393–1442, 1987. 794
Beck, M. B., Ravetz, J. R., Mulkey, L. A., and Barnwell, T. O.: On the problem of model validation for predictive exposure assessments, Stoch. Hydrol. Hydraul., 11, 229–254, 1997. 793
Bertoldi, G., Rigon, R., and Over, T. M.: Impact of watershed geomorphic characteristics on the energy and water budgets, J. Hydrometeorol., 7, 389–403, 2006. 796
Beven, K.: Prophecy, reality and uncertainty in distributed hydrological modelling, Adv. Water Resour., 16, 41–51, 1993. 793, 794
Beven, K. and Binley, A.: The future of distributed models: model calibration and uncertainty prediction, Hydrol. Process., 6, 279–298, 1992. 794, 813
Beven, K. and Freer, J.: Equifinality, data assimilation, and uncertainty estimation in mechanistic modelling of complex environmental systems using the GLUE methodology, J. Hydrol., 249, 11–29, 2000. 812
Brutsaert, W.: On a derivable formula for long-wave radiation from clear skies, Water Resour. Res., 11, 742–744, 1975. 799
Carey, S. K., Quinton, W. L., and Goeller, N. T.: Field and laboratory estimates of pore size properties and hydraulic characteristics for subarctic organic soils, Hydrol. Process., 21, 2560–2571, doi:10.1002/hyp.6795, 2007. 803
Cermák, V. and Rybach, L.: Thermal conductivity and specific heat of minerals and rocks, in: Landolt-Börnstein Zahlenwerte und Funktionen aus Naturwissenschaften und Technik, Physikalische Eigenschaften der Gesteine, Springer, New York, 305–343, 1982. 803
Chen, M. H., Shao, Q. M., and Ibrahim, J. G.: Monte Carlo Methods in Bayesian Computation, Springer Verlag, New York, 2000. 794
Crosetto, M. and Tarantola, S.: Uncertainty and sensitivity analyses: tools for GIS-based model implementation, Int. J. Geograph. Inf. Sci., 15, 415–437, 2001. 794
Cukier, R. I., Levine, H. B., and Shuler, K. E.: Nolinear sensitivity analysis of multiparameter model systems, J. Phys. Chem., 81, 2365–2366, 1977. 794

GMDD
6, 791–840, 2013

Dall'Amico, M.: Coupled water and heat transfer in permafrost modeling, Ph.D. Thesis, Institute of Civil and Environmental Engineering, Universita degli Studi di Trento, Trento, 2010. 796, 798

Davis, T. J. and Keller, C. P.: Modelling uncertainty in natural resource analysis using fuzzy sets and Monte Carlo simulation: slope stability prediction, Geogr. Inf. Sci., 11, 409–434, 1997. 794

Dozier, J. and Warren, S. G.: Effect of viewing angle on the infrared brightness temperature of snow, Water Resour. Res., 18, 1424–1434, 1982. 801

Endrizzi, S.: Snow cover modelling at local and distributed scale over complex terrain, Ph.D. thesis, Institute of Civil and Environmental Engineering, Universita degli Studi di Trento, Trento, 2007. 796

Essery, R. and Etchevers, P.: Parameter sensitivity in simulation of snowmelt, J. Geophys. Res., 109, D20111, doi:10.1029/2004JD005036, 2004. 812, 813

Etchevers, P., Martin, E., Brown, R., Fierz, C., Lejeune, Y., Bazile, E., Boone, A., Dai, Y. J., Essery, R., Fernandez, A., Gusev, Y., Jordan, R., Koren, V., Kowalczyk, E., Nasonova, N. O., Pyles, R. D., Schlosser, A., Shmakin, A. B., Smirnova, T., Strasser, U., Verseghy, D., Yamazaki, T., and Yang, Z. L.: Validation of the energy budget of an alpine snowpack simulated by several snow models (SnowMIP project), Ann. Glaciol., 38, 150–158, 2004. 813

Etzelmüller, B., Hoelzle, M., Heggem, E. S. F., Isaksen, K., Stocker-Mittaz, C., Ødegård, R. S., Haeberli, W., and Sollid, J. L.: Mapping and modelling the occurrence and distribution of mountain permafrost, Norsk Geograf. Tidsskr., 55, 186–194, 2001. 830

Gold, L. W. and Lachenbruch, A. H.: Thermal conditions in permafrost – a review of North American literature, in: Proceedings of the 2nd International Conference on Permafrost, Yakutsk, USSR, 3–25, 13–28 July 1973. 811

Goodison, B. E., Louie, P. Y. T., and Yang, D.: WMO solid precipitation measurement intercomparison, Tech. Rep., World Meteorological Organization, Geneva, Switzerland, 1998. 801

Goodrich, L. E.: The influence of snow cover on the ground thermal regime, Can. Geotech. J., 19, 421–432, doi:10.1139/t82-047, 1982. 804, 812

Gruber, S.: Mountain Permafrost: Transient Spatial Modelling, Model Verification and the Use of Remote Sensing, Ph.D. thesis, University of Zurich, Zurich, 2005. 813

Gruber, S. and Hoelzle, M.: The cooling effect of coarse blocks revisited: a modeling study of a purely conductive mechanism, in: 9th International Conference on Permafrost, Fairbanks, Alaska, 557–561, 28 June –3 July 2008. 795

GMDD
6, 791–840, 2013

Gubler, S., Fiddes, J., Keller, M., and Gruber, S.: Scale-dependent measurement and analysis of ground surface temperature variability in alpine terrain, The Cryosphere, 5, 431–443, doi:10.5194/tc-5-431-2011, 2011. 795, 797, 804, 806, 811, 814, 832

Gubler, S., Gruber, S., and Purves, R. S.: Uncertainties of parameterized surface downward clear-sky shortwave and all-sky longwave radiation., Atmos. Chem. Phys., 12, 5077–5098, doi:10.5194/acp-12-5077-2012, 2012. 799, 801, 806, 813

Gupta, H. V., Sorooshian, S., and Patrice, O. Y.: Toward improved calibration of hydrologic models: Multiple and noncommensurable measures of information, Water Resour. Res., 34, 751–763, 1998. 813

Gupta, H. V., Beven, K., and Wagener, T.: Model Calibration and Uncertainty Estimation, John Wiley & Sons, New York, 2005. 793, 794, 829

Gupta, H. V., Wagener, T., and Liu, Y.: Reconciling theory with observations: elements of a diagnostic approach to model evaluation, Hydrol. Process., 22, 3802–3813, 2008. 812, 815

Haeberli, W.: Die Basis-Temperatur der winterlichen Schneedecke als möglicher Indikator für die Verbreitung von Permafrost in den Alpen, Z. Gletscherk. Glaziol., 9, 221–227, 1973. 795

He, M., Hogue, T. S., Franz, K. J., Margulis, S. A., and Vrugt, J. A.: Characterizing parameter sensitivity and uncertainty for a snow model across hydroclimatic regimes, Adv. Water Resour., 34, 114–127, 2011. 812

Hoelzle, M.: Mapping and modelling of mountain permafrost distribution in the Alps, Norsk Geograf. Tidsskr., 50, Ho11–15, 1996. 795, 813

Hoelzle, M., Mittaz, C., Etzelmüller, B., and Haeberli, W.: Surface energy fluxes and distribution models of permafrost in European mountain areas: an overview of current developments, Permafrost Periglac. Process., 12, 53–68, 2001. 830

Hoelzle, M., Haeberli, W., and Mittaz, C.: Miniature ground temperature data logger measurements 2000–2002 in the Murtèl-Corvatsch area, Eastern Swiss alps, in: 8th International Conference on Permafrost, Proceedings, edited by: Phillips, M., Springman, S., and Arenson, L., Swets & Zeitlinger, Lisse, Zürich, 419–424, 21–25 July 2003. 795

Hori, M., Aoki, T., Tanikawa, T., Motoyoshi, H., Hachikubo, A., Siugiura, K., Yasunari, T. J., Eide, H., Storvold, R., Nakajima, Y., and Takahashi, F.: In-situ measured spectral directional emissivity of snow and ice in the 8–14 µm atmospheric window, Remote Sens. Environ., 100, 486–502, 2006. 801

Idso, S. B.: A set of equations for full spectrum and 8 to 14 µm and 10.5 to 12.5 µm thermal radiation from cloudless skies, Water Resour. Res., 17, 295–304, 1981. 799

Ineichen, P., Guisan, O., and Perez, R.: Ground-reflected radiation and albedo, Solar Energy, 44, 207–214, 1990. 800
Ishikawa, M.: Thermal regine at the snow-ground interface and their implications for permafrost investigation, Geomorphology, 52, 105–120, 2003. 812
Jhorar, R. K., Bastiaanssen, W. G. M., Feddes, R. A., and Van Dam, J. C.: Inversely estimating soil hydraulic functions using evapotranspiration fluxes, J. Hydrol., 258, 198–213, 2002. 814
Jin, M. and Shunlin, L.: An improved land surface emissivity parameter for land surface models using global remote sensing observations, J. Climate, 19, 2867–2881, 2006. 800
Keller, F. and Gubler, H. U.: Interaction between snow cover and high mountain permafrost at Murtél Corvatsch, Swiss Alps, in: The Sixth International Conference on Permafrost, Beijing, 332–337, 1993, 5-9 JULY. 795, 812
Kelley, C. T.: Solving Nonlinear Equations with Newton's method, Society for Industrial and Applied Mathematics, SIAM, Philadelphia, USA, 2003. 798
Kohl, T.: Transient thermal effects below complex topographies, Tectonophysics, 306, 311–324, 1999. 800
Konzelmann, T., van de Wal, R. S. W., Greuell, W., Bintanja, R., Henneken, E. A. C., and Abe-Ouchi, A.: Parameterization of global and longwave incoming radiation for the Greenland Ice Sheet, Global Planet. Change, 9, 143–164, 1994. 799, 808, 813
Legates, D. R. and DeLiberty, T. L.: Precipitation measurement biases in the United States, J. Am. Water Resour. Assoc., 29, 855–861, doi:10.1111/j.1752-1688.1993.tb03245.x, 1993. 801
Ling, F. and Zhang, T.: A numerical model for surface energy balance and thermal regime of the active layer and permafrost containing unfrozen water, Cold Reg. Sci. Technol., 38, 1–15, 2004. 813
Luetschg, M., Lehning, M., and Haeberli, W.: A sensitivity study of factors influencing warm/thin permafrost in the Swiss Alps, J. Glaciol., 54, 696–704, 2008. 795, 812
Maier, U., de Biase, C., Baeder-Bederski, O., and Bayer, P.: Estimation of Van Genuchten and preferential flow parameters by inverse modelling for large scale vertical flow constructed wetlands, in: EGU General Assembly, Geophys. Res. Abstr., p.12916, Vienna, Austria, 2009. 803
Markvart, T. and Castañer, L.: Practical Handbook of Photovoltaics: Fundamentals and Applications, Elsevier, Amsterdam, 2003. 800, 801

GMDD
6, 791–840, 2013

Medici, F. and Rybach, L.: Geothermal map of Switzerland 1995 (heat flow density), Matériaux pour la Géologie de la Suisse, Géophysique Nr. 30, Schweizerische Geophysikalische Kommision, 1995. 800

Mertens, J., Madsen, H., Kristensen, M., Jaques, D., and Feyen, J.: Sensitivity of soil parameters in unsaturated zone modeling and the relation between effective, laboratory and in situ measurements, Hydrol. Process., 19, 1611–1633, 2005. 814

Monin, A. S. and Obukhov, A. M.: Basic laws of turbulent mixing in the surface layer of the atmosphere, Tr. Akad. Nauk SSSR Geophiz. Inst., 24, 163–187, 1954. 799

Nötzli, J., Gruber, S., Kohl, T., Salzmann, N., and Haeberli, W.: Three-dimensional distribution and evolution of permafrost temperatures in idealized high-mountain topography, J. Geophys. Res., 112, F02S13, doi:10.1029/2006JF000545, 2007. 800

Obukhov, A. M.: Turbulence in an atmosphere with a non-uniform temperature, Bound.-Layer Meteorol., 2, 7–29, 1946. 799

Ogawa, K. and Schmugge, T.: Mapping surface broadband emissivity of the Sahara desert using ASTER and MODIS data, Earth Interact., 8, 1–14, doi:10.1175/1087-3562(2004)008<0001:MSBEOT>2.0.CO;2, 2004. 800

Pollaco, J. A. P. and Mohanty, B. P.: Uncertainties of water fluxes in soil-vegetation-atmosphere transfer models: inverting surface soil moisture and evapotranspiration retrieved from remote sensing, Vadose Zone J., v. 11, vzj2011.0167, doi:10.2136/?vzj2011.0167, 2012. 814

Polo, J., Martín, L., and Cony, M.: Revision of ground albedo estimation in Heliosat scheme for deriving solar radiation from SEVIRI HRV channel of Meteosat satellite, Solar Energy, 86, 275–282, 2012. 800

Prata, A. J.: A new long-wave formula for estimating downward clearsky radiation at the surface, Q. J. R. Meteorol. Soc., 122, 1127–1151, 1996. 799

Quinton, W. L., Hayashi, M., and Carey, S. K.: Peat hydraulic conductivity in cold regions and its relation to pore size and geometry, Hydrol. Process., 22, 2829–2837, doi:10.1002/hyp.7027, 2008. 803

Rigon, R., Bertoldi, G., and Over, T. M.: GEOtop: a distributed hydrological model with coupled water and energy budget, J. Hydrometeorol., 7, 371–388, 2006. 796, 803

Romanovsky, V. E., Osterkamp, T. E., and Duxbury, N. S.: An evaluation of three numerical models used in simulations of the active layer and permafrost temperature regimes, Cold Reg. Sci. Technol., 26, 195–203, 1997. 813

Rykiel, J. E. J.: Testing ecological models: the meaning of validation, Ecol. Model., 90, 299–244, 1996. 793
Saltelli, A., Tarantola, S., and Campolongo, F.: Sensitivity Analyses in Practice, doi:10.1002/0470870958, John Wiley and Sons, New York, 2004. 794
Saltelli, A., Ratto, M., Andres, T., Campolongo, F., Cariboni, J., Gatelli, D., Saisana, M., and Tarantola, S.: Global Sensitivity Analysis. The Primer, John Wiley & Sons, New York, 2008. 794
Scharmer, K. and Greif, J.: The European Solar Radiation Atlas, Vol. 1: Fundamentals and Maps, Les Presses de l'École des Mines, Paris, France, 2000. 800
Schmid, M.-O., Gubler, S., Fiddes, J., and Gruber, S.: Inferring snowpack ripening and melt-out from distributed measurements of near-surface ground temperatures, The Cryosphere, 6, 1127–1139, doi:10.5194/tc-6-1127-2012, 2012. 797, 804, 806, 832
Seaman, J., Singer, J., and Aburime, S.: Evaluating the relative importance of the van Genuchten–Mualem parameters, in: Proceedings of the 2009 Georgia Water Resources Conference, 27–29 April 2009. 814
Sobol, I. M.: Sensitivity analysis for non-linear mathematical model, Math. Model. Comput. Exp., 1, 407–414, 1993. 794
Stow, C., Jollif, J., McGillicuddy Jr., D. J., Doney, S. C., Allen, J. I., Friedrichs, M. A. M., Rose, K. A., and Wallhead, P.: Skill assessment for coupled biological/physical models of marine systems, J. Mar. Syst., 76, 4–15, 2009. 793
Sutherland, R. A.: Broadband and spectral emissivities (2–18 µm) of some natural soils and vegetation, J. Atmos. Ocean. Technol., 3, 199–202, 1986. 800
Tarboton, D. G. and Luce, C. H.: Utah Energy Balance Snow Accumulation and Melt Model (UEB), Tech. rep., Utah Water Research Laboratory Utah State University and USDA Forest Service Intermountain Research Station, Utah, USA, 1996. 801
Tetzlaff, G.: Albedo of the Sahara, in: Satellite measurements of radiation budget parameters, edited by: Raschke, E., 60–63, Bonn, 1983. 800
Tufte, E.: The Visual Display of Quantitative Information, Graphics Press, Cheshire, Connecticut, USA, 1983. 806
Tufte, E.: Envisioning Information, Graphics Press, Cheshire, Connecticut, USA, 1990. 806
Twarakavi, N. K. C., Simunek, J., and Schaap, M. G.: Can texture-based classification optimally classify soils with respect to soil hydraulics?, Water Resour. Res., 46, doi:10.1029/2009WR007939, 2010. 803

GMDD
6, 791–840, 2013

van Genuchten, M. T.: A closed-form equation for predicting the hydraulic conductivity of unsaturated soils, Soil Sci. Soc. Am. J., 44, 892–898, 1980. 802

Šafanda, J.: Ground surface temperature as a function of the slope angle, Tectonophysics, 360, 367–375, 1999. 803

Wegmann, M., Gudmundsson, G. H., and Haeberli, W.: Permafrost changes in rock walls and the retreat of Alpine glaciers: a thermal modelling approach, Permafrost Periglac. Process., 9, 23–33, 1998. 803

Wieringa, J.: Representative roughness parameters for homogeneous terrain, Bound.-Layer Meteorol., 63, 323–363, 1993. 800

Williams, P. and Smith, M.: The Ground Thermal Regime, Chap. 4, Cambridge University Press, Cambridge, 83–121, 1989. 795, 802

Zhang, T.: Influence of the seasonal snow cover in the ground thermal regime: an overview, Rev. Geophys., 43, doi:10.1029/2004RG000157, 2005. 801, 804

GMDD
6, 791–840, 2013

Table 1. Parameters selected for the sensitivity study. The minimum and the maximum indicate the range from which the parameters are sampled, the base indicates the standard choice used in e.g. local sensitivity studies. The right part indicates the prior distributions of the parameters considered in the uncertainty analysis.

Parameter	Symbol	Unit	Base	Sensitivity		Uncertainty		
				Min	Max	Distr.	Par_1	Par_2
Numerical parameter								
Thickness of first ground layer	dz_{min}	mm	20	5	640			
Growth rate ground depth	b		0.5	0	1			
Maximal ground depth	z_{max}	m	10	1.25	20			
Number of top snow layers	n_t		4	1	10			
Number of bottom snow layers	n_b		2	1	10			
Number of snow layers in middle	n_m		4	1	64			
Typical SWE	swe_m	mm	10	1.25	40			
Time discretization	dt	h	1	0.125	4			
Richard's tolerance	tol_r	mm	10^{-4}	10^{-8}	10^{-4}			
Heat equation tolerance	tol_h	$J\,m^{-2}$	10^{-4}	10^{-8}	10^{-4}			
Model parameter								
Minimal wind velocity	V_{min}	$m\,s^{-1}$	0.5	0.01	1.28			
Minimal relative humidity	RH_{min}	%	10	1	10			
LDR calibration	$LDR_{in,K}$							
Monin–Obukhov param.	MO		1	1	4			
Water balance	WB		1	0	1			
Physical parameter								
Initial Ground Temperature	T_i	°C	1	−1	1			
Depth above which water drains	z_f	m	10	0.01	10	Unif	0	10
Extinction parameter snow albedo	c_α	mm	10	0	200	Log-N	1.71	1.09
Ground roughness	r_g	mm	10	0.01	100	Log-N	1.96	0.83
Dry ground albedo	$\alpha_{g,dry}$		0.2	0.1	0.4	Norm	0.25	0.05
Divisor wet ground albedo	$f_{\alpha_{g,wet}}$		1	1	2.5	Norm	1.75	0.25
Ground emissivity	ϵ_g		0.96	0.81	0.99	Norm	0.93	0.02
Ground heat flux	Q_g	$W\,m^{-2}$	0.05	−0.1	0.1			
Snow roughness	r_s	mm	0.1	0.01	10	Log-N	−2.64	0.83
Fresh snow albedo (vis)	$\alpha_{s,\,vis}$		0.96	0.8	0.96	Norm	0.93	0.02
Fresh snow albedo (nir)	$\alpha_{s,\,NIR}$		0.65	0.6	0.7	Norm	0.65	0.02
Snow emissivity	ϵ_s		0.98	0.96	0.99			
Snow viscosity	ν_s	$N\,s\,m^{-2}$	10^6	10^6	8×10^6	Norm	4×10^6	2×10^6
Ground-snow roughness threshold	$c_{s,r}$	mm	1	0.5	1			
Irreducible water saturation snow	$s_{w,irr}$		0.02	0.005	0.08	Log-N	−4.02	0.47
Snow density cutoff	$d_{s,\,cut}$	$kg\,m^{-3}$	100	75	175	Log-N	4.58	0.2
Dry snow deformation rate	$df_{s,\,dry}$	%	1	0.75	1.25			
Wet snow deformation rate	$df_{s,\,wet}$	%	1.5	1.25	2.5			
Temperature threshold rain	$T_{r,0}$	°C	3	0	4	Norm	2	0.5
Temperature threshold snow	$T_{s,0}$	°C	−1	−3	0	Norm	−1.75	0.5
Ozone	O_3	mm	0.314	0.238	0.39			
Ångström α	$\alpha_{Å}$		1.38	0.46	2.30			
Ångström β	$\beta_{Å}$		0.039	0.010	0.139	Log-N	−3.73	0.99
Albedo to determine SDR	α_c		0	0	1			

GMDD
6, 791–840, 2013

Table 2. Second part of Table 1.

Parameter	Symbol	Unit	Base	Sensitivity		Uncertainty		
				Min	Max	Distr.	Par_1	Par_2
Residual water content (F)	$f_{\theta_{res}}$		1	0.8	1.2			
Saturated water content (F)	$f_{\theta_{sat}}$		1	0.9	1.1	Norm	1	0.05
van Genuchten parameter α (F)	$f_{\alpha_{vG}}$		1	0.75	1.25			
van Genuchten parameter n (F)	$f_{n_{vG}}$		1	0.5	1.5	Norm	1	0.25
Hydraulic conductivity (F)	f_{K_h}		1	0.01	100	Norm	0	1
Thermal capacity (F)	f_C		1	0.8	1.2			
Thermal conductivity (F)	f_{K_T}		1	0.5	1.5	Norm	1	0.25
Input								
Temperature lapse rate	Γ_T	$^\circ C\,km^{-1}$	6.5	5.5	7.5			
Dew temperature lapse rate	Γ_{DT}	$^\circ C\,km^{-1}$	2.5	1.5	3.5			
Precipitation lapse rate	Γ_P	km^{-1}	0.2	−0.1	0.3			
Correction factor for precip.	c_P		2	1.6	2.4			
Sensor height wind velocity	h_w	m	2	0.5	16	Log-N	0.66	0.25
Sensor height temperature	h_T	m	2	0.5	16	Log-N	0.66	0.25

GMDD
6, 791–840, 2013

Table 3. Environmental attributes determining the locations for which the sensitivity and uncertainty analyses are performed. The sky view factor (SVF) is a function of slope. For each combination of attributes, a separate sensitivity and uncertainty analysis is performed, resulting in a total of 200 simulation locations per ground type (respectively 328 for rock). In total, 1328 sensitivity and uncertainty analyses were performed.

Attribute	Unit	Min	Max	Step
Elevation	m	500	4000	500
Aspect	deg	0	360	45
Slope	deg	0	30	10
SVF		0.93	1	
Ground		1	6	e.g. Table 4

GMDD
6, 791–840, 2013

Table 4. Parameters of the different ground types. In the sensitivity analysis, the hydraulic parameters are assumed to change by ±20 % for θ_{sat}, ±10 % for θ_{res}, ±50 % for n_{vG}, ±25 % for α_{vG}, and goes from 0.01 to 100 times the original value for K_h. The thermal conductivity changes by 50 % and the heat capacity changes by 20 % (i.e. Table 1). The values are modified by the respective factors presented in Table 1.

Parameter	Symbol	Unit	Clay	Silt	Sand	Peat	Gravel	Rock
Residual water content	θ_r		0.072	0.057	0.055	0.2	0.055	0.002
Saturated water content	θ_s		0.475	0.487	0.374	0.85	0.374	0.05
van Genuchten α	α_{vG}	mm^{-1}	0.001	0.001	0.003	0.03	0.1	0.001
van Genuchten n	n_{vG}		1.4	1.6	3.2	1.8	2	1.2
Hydraulic conductivity	K_h	$mm\ s^{-1}$	0.0019	0.0051	0.0825	0.3	10	0.000001
Thermal conductivity	K_T	$W\ m^{-1}\ K^{-1}$	2.5	–	–	–	–	–
Thermal capacity	C	$J\ m^{-3}\ K^{-1}$	2.25×10^6	–	–	–	–	–

GMDD
6, 791–840, 2013

Table 5. Average discretization error ε [°C] of MAGT modeled at 1 m depth due to the different discretization parameters.

dt	1800	3600	7200	14 400							
ε_{dt}	0	0.027	0.113	0.226							
n_m	64	32	16	8	4	2	1				
ε_{n_m}	0	0	0	0.001	0.013	0.004	0.023				
swe_m	1.25	2.5	5	10	20	40					
$\varepsilon_{\mathrm{swe}_m}$	0	−0.025	−0.032	−0.02	0.093	0.225					
n_b	10	9	8	7	6	5	4	3	2	1	
ε_{n_b}	0	0	0	0	0	0	0	0	0	0.001	
n_t	10	9	8	7	6	5	4	3	2	1	
ε_{n_t}	0	0	0	0	0	0.001	0.002	0.004	0.004	0.172	
$dz_{\min}$	5	10	20	40	80	160	320	640			
$\varepsilon_{dz_{\min}}$	0	0.061	0.138	0.231	0.444	0.749	1.11	1.535			
$z_{\max}$	20 000	10 000	5000	2500	1250						
$\varepsilon_{z_{\max}}$	0	−0.004	−0.001	−0.002	−0.098						
b	1	1.1	1.2	1.3	1.4	1.5	1.6	1.7	1.8	1.9	2
ε_b	0	−0.001	0.002	0.001	−0.006	−0.003	−0.001	−0.001	−0.033	−0.022	−0.014

GMDD
6, 791–840, 2013

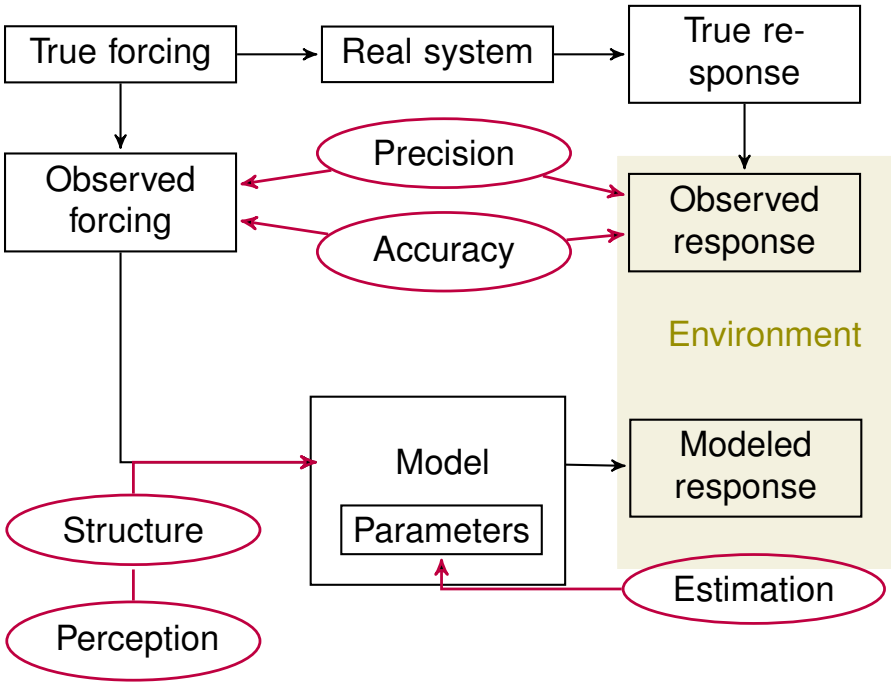

Fig. 1. Model uncertainties and errors has diverse sources (red) such as unknown parameters, errors in input data, numerical errors due to discretization, etc. Uncertainty and sensitivity studies investigate the effect of these possible sources of errors on model outputs (adapted from Gupta et al., 2005). Observed and modeled responses as well as model sensitivities are subject to strong environmental variation.

GMDD
6, 791–840, 2013

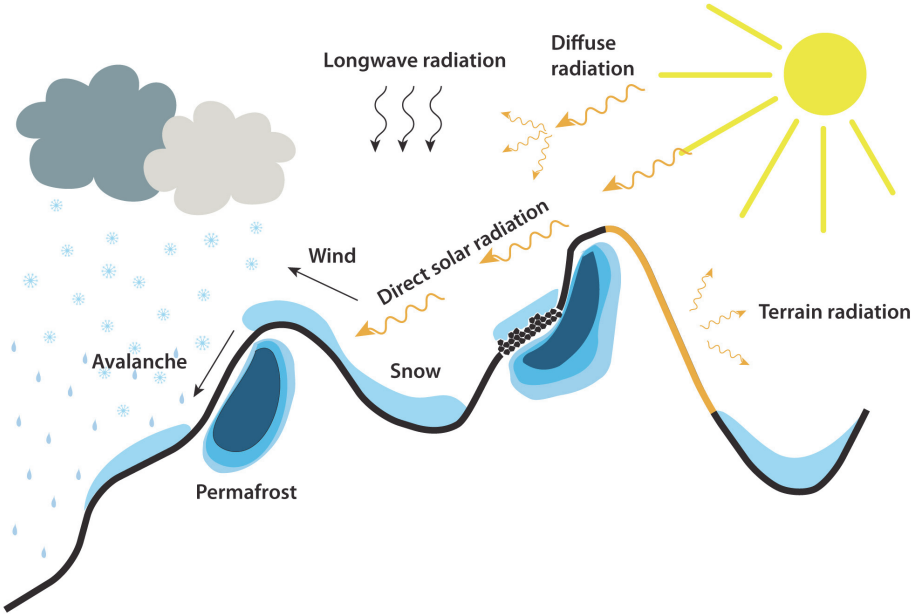

Fig. 2. Processes that influence permafrost are highly variable in mountain areas. The energy balance, shading from surrounding terrain and snow redistribution by wind or avalanches influence permafrost occurrence in high mountain. The scale determines the importance of the influencing processes (Etzelmüller et al., 2001; Hoelzle et al., 2001).

GMDD
6, 791–840, 2013

Fig. 3. The height of the meteorological station at Corvatsch is assumed uncertain, ranging from 0.5 to 16 m. Within mountain topography, the actual height in relation with the surroundings at the top of a mountain cannot be accurately determined. In the figure, the meteorological station is just above the "tsch" of "Corvatsch".

GMDD
6, 791–840, 2013

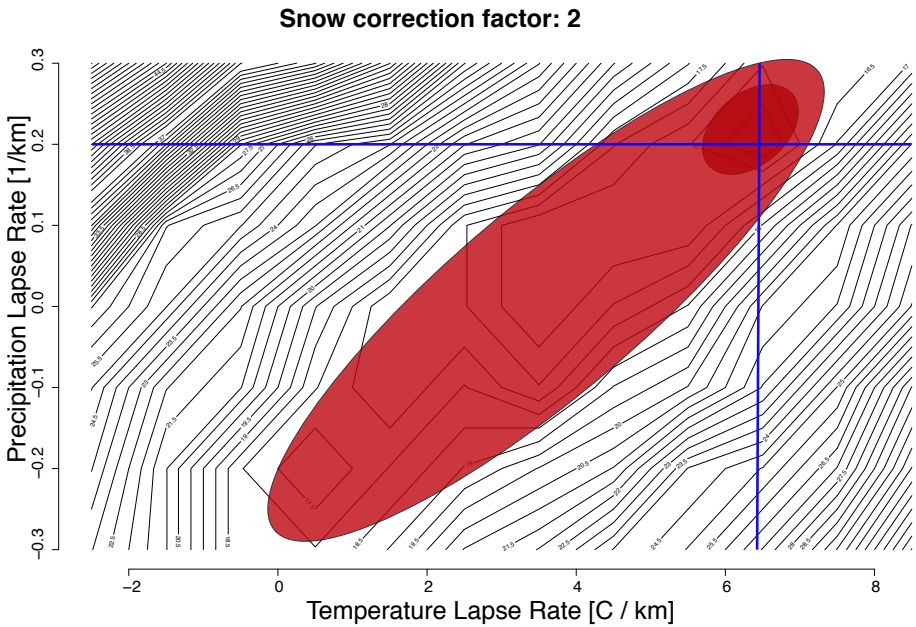

Fig. 4. Contour plot of the RMSD for simulated compared to observed MD around Piz Corvatsch, Switzerland (Gubler et al., 2011; Schmid et al., 2012). The smallest RMSD are obtained for a a temperature lapse rate 6.5 °C km^{-1}, a snow correction factor of 2 and a precipitation lapse rate of 0.2 km^{-1} (indicated by the blue lines).

GMDD
6, 791–840, 2013

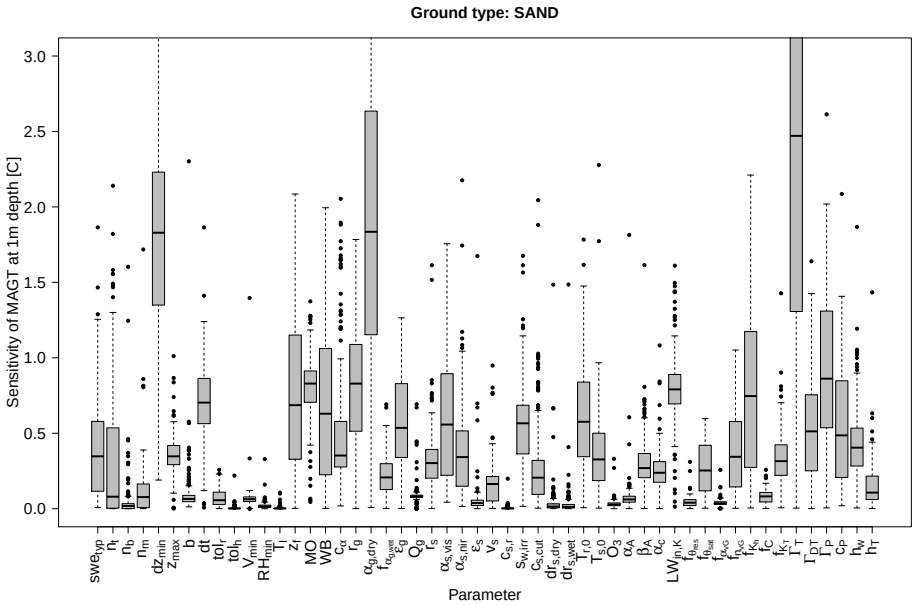

Fig. 5. Sensitivities of the target variable MAGT at 1 m depth [°C] for sandy ground. The sensitivities of the topographic locations are summarized as boxplots. The greater the spread of the box, the higher the variability of the sensitivity within the topographic setting The range of the boxplots is equivalent to the "potential of being mislead" by the results of a sensitivity analysis performed at one single location. See Table 1 for an explanation of parameter names.

GMDD
6, 791–840, 2013

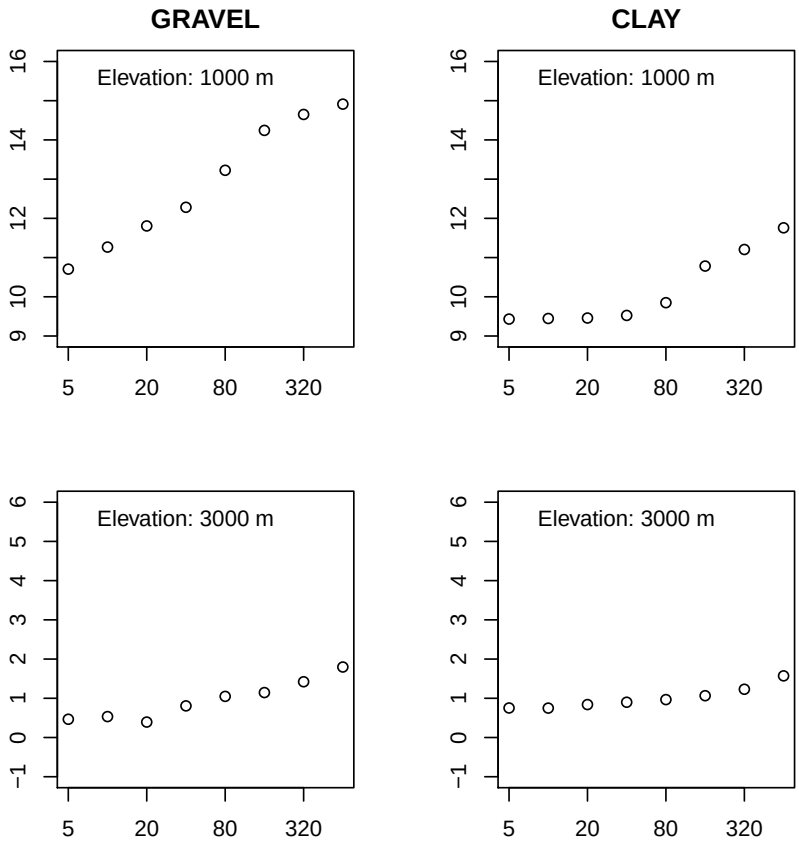

Fig. 6. Sensitivities of MAGT modeled at 10 cm depth to the thickness of the first ground layer for gravel (left) and clay (right). Modeled MAGT in gravel increase linearly for increasing ground thickness (note the logarithmic x-axis), while MAGT in clay are constant for $dz_{\min} \leq 20$ mm. The sensitivity to $dz_{\min}$ decreases for ground temperatures closer to zero degree Celsius (bottom figures).

GMDD
6, 791–840, 2013

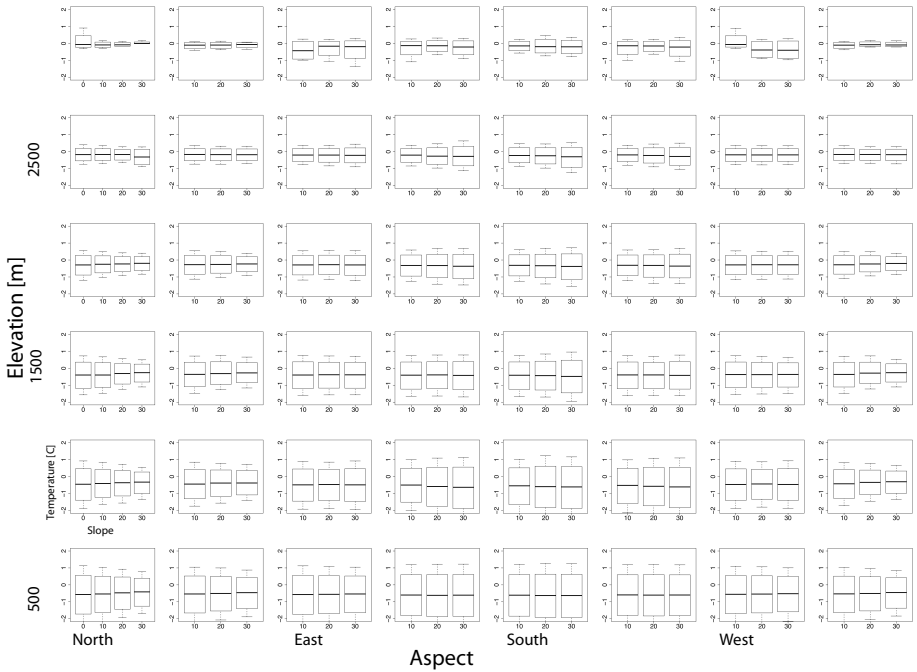

Fig. 7. Small multiple plots of normalized boxplots of MAGT at 1 m depth [°C], simulated at all topographic locations for different ground albedo values. The boxplots represent the different model outputs. The length of the 95 % uncertainty range of each boxplot indicates the sensitivity to dry ground albedo at each location.

GMDD
6, 791–840, 2013

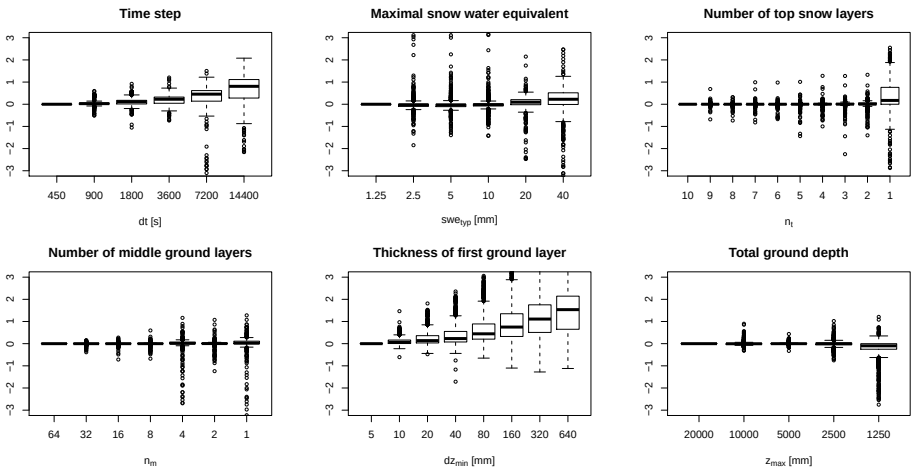

Fig. 8. Sensitivities of MAGT modeled at 1 m depth to the six sensitive discretization parameters dt (top left), swe_m (top middle), n_t (top right), n_m (bottom left), dz_{min} (bottom middle) and z_{max} (bottom right), normalized with MAGT modeled with the finest resolution of each parameter. The sensitivities are summarized as boxplots for all topographic properties and the six ground types.

GMDD
6, 791–840, 2013

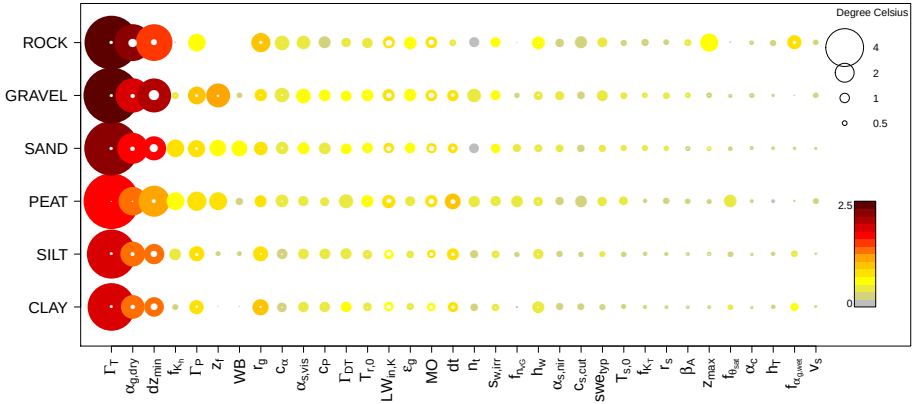

Fig. 9. Sensitivities of topographic sensitivity summarized as the 5 %, 50 % and 95 % percentiles of MAGT modeled at 1 m depth for all ground types. The area of the circle indicates the 95 % percentile, and the area of the white dot the 5 % percentile of the sensitivity, summarized for all topographic locations. The color indicates the median sensitivity.

GMDD
6, 791–840, 2013

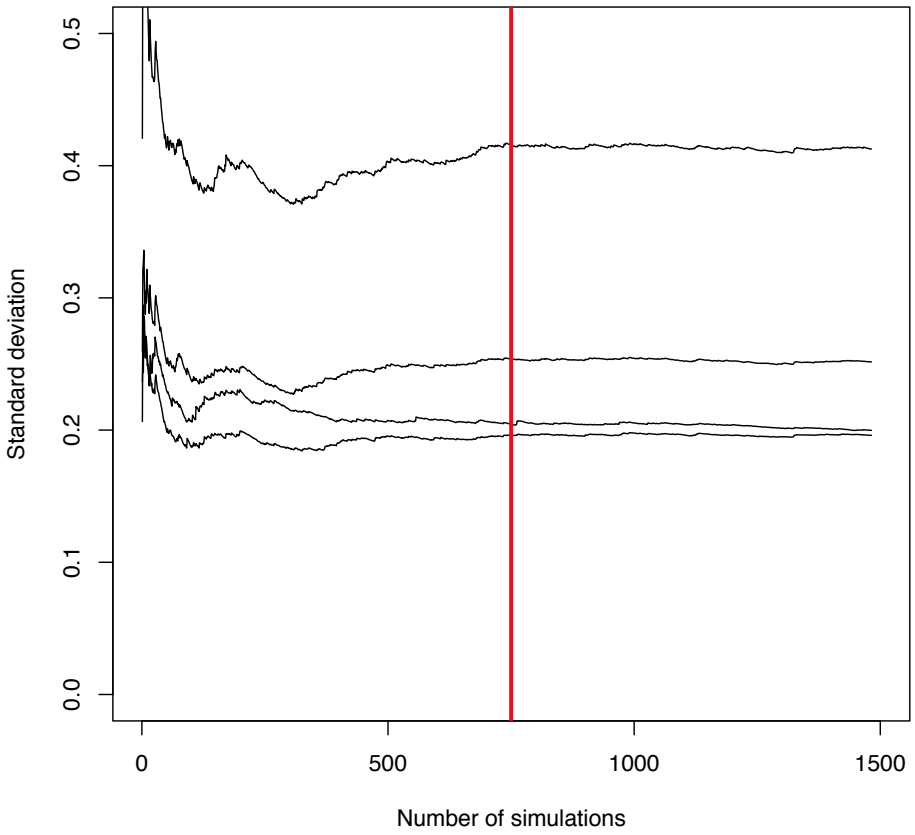

Fig. 10. Standard deviation of the model MAGT at 10 cm depth for increasing number of simulations (sand) at four arbitrarily selected points. Convergence is reached at approximately 750 simulations (indicated by the red line).

GMDD
6, 791–840, 2013

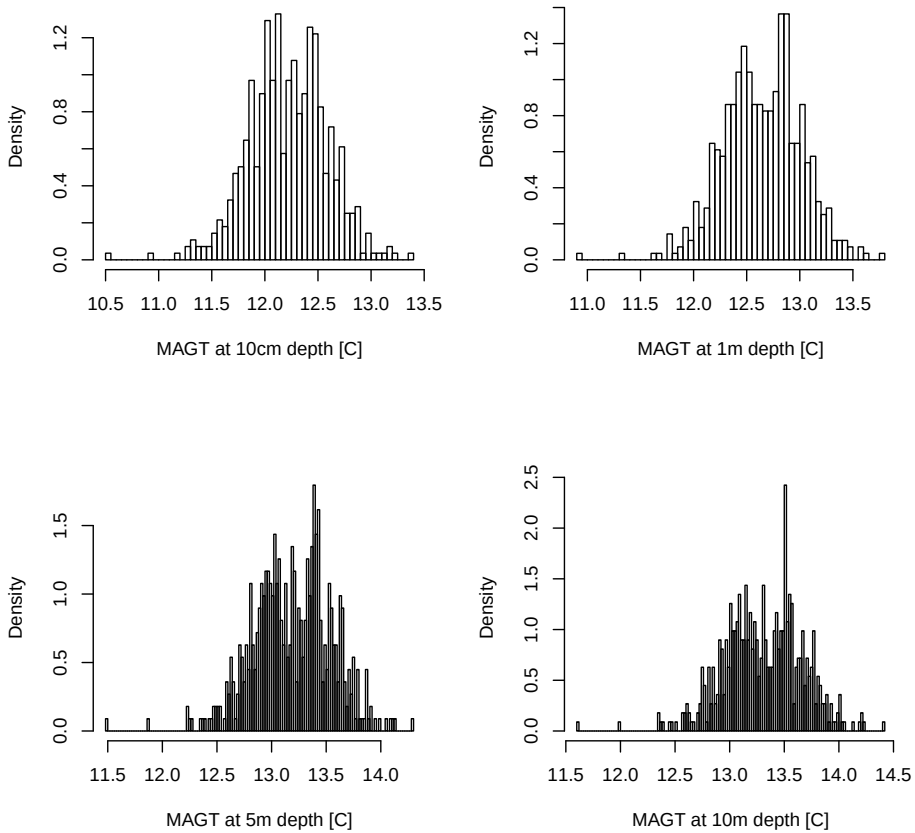

Fig. 11. Density histograms of modeled MAGT at the four depths for 1500 simulations. The uncertainty depicted in Fig. 12 is defined as the standard deviation of the simulated MAGT as shown here.

GMDD
6, 791–840, 2013

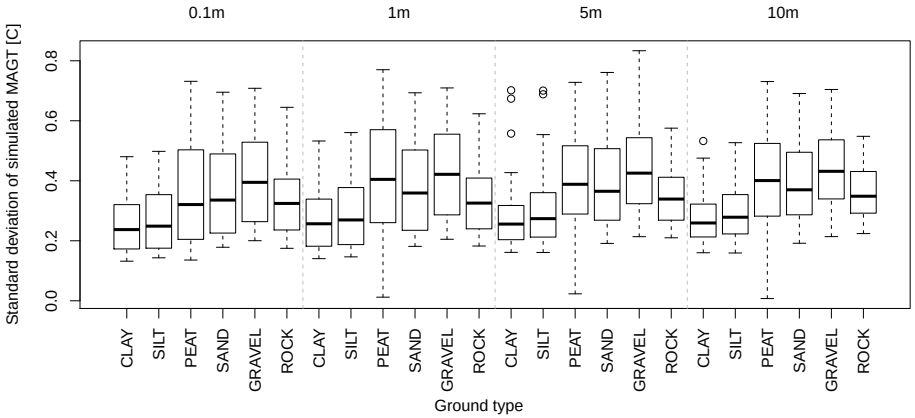

Fig. 12. Boxplots for all topographic locations of total output uncertainty of MAGT expressed as a standard deviation, presented for all ground types and depths. The parametric uncertainty is increased for sand, peat and gravel, i.e. for the ground types for which the hydraulic properties are sensitive (e.g. Sect. 4.2).

GMDD
6, 791–840, 2013